Research Article

Land Cover Information Extraction Based on Daily NDVI Time Series and Multiclassifier Combination

Long Zhao,[1] Pan Zhang,[2] Xiaoyi Ma,[2] and Zhuokun Pan[3]

[1]*College of Mechanical and Electronic Engineering, Northwest A&F University, Yangling, Shaanxi Province 712100, China*
[2]*College of Water Resources and Architectural Engineering, Northwest A&F University, Yangling, Shaanxi Province 712100, China*
[3]*College of Natural Resources and Environment, South China Agricultural University, Guangzhou, Guangdong Province 510000, China*

Correspondence should be addressed to Xiaoyi Ma; xma@nwafu.edu.cn

A timely and accurate understanding of land cover change has great significance in management of area resources. To explore the application of a daily normalized difference vegetation index (NDVI) time series in land cover classification, the present study used HJ-1 data to derive a daily NDVI time series by pretreatment. Different classifiers were then applied to classify the daily NDVI time series. Finally, the daily NDVI time series were classified based on multiclassifier combination. The results indicate that support vector machine (SVM), spectral angle mapper, and classification and regression tree classifiers can be used to classify daily NDVI time series, with SVM providing the optimal classification. The classifiers of K-means and Mahalanobis distance are not suited for classification because of their classification accuracy and mechanism, respectively. This study proposes a method of dimensionality reduction based on the statistical features of daily NDVI time series for classification. The method can be applied to land resource information extraction. In addition, an improved multiclassifier combination is proposed. The classification results indicate that the improved multiclassifier combination is superior to different single classifier combinations, particularly regarding subclassifiers with greater differences.

1. Introduction

Land use and land cover change have been recognized as major factors in human activities affecting regional change and biological systems [1, 2]. Land cover information can provide a basis for formulating ecological protection measures and implementing sustainable development [3–5]. Remote-sensing technology has become the primary means of land cover information acquisition and has the advantages of high data acquisition speed, high updating speed, wide range, economic convenience, and rich spatial information [6–8].

With the continuous development of remote-sensing technology, the image space and time resolution of remote sensing are continually increasing, and remote-sensing image processing is presenting new challenges. The methods for classification commonly used in remote-sensing images include maximum likelihood [9], minimum distance [10], object-oriented [11], spectral angle mapper (SAM) [12], support vector machine (SVM) [13], and neural networking [14, 15] classifiers. Giacinto and Roli [16] conducted a comparative study of the application of various classifiers in remote-sensing data classification, the results of which indicated that no classifier is universal. In addition to the development of more advanced classifiers, multiclassifier combinations are one approach to improving classification accuracy, because different classifiers can provide complementary information on the images to be classified [17]. This combinatorial approach can obtain higher accuracy than any single classifier. Habibi et al. [18] proved that in segment-based classification multiple classifiers achieved higher overall accuracy. However, in multiclassifier combinations, each classifier predicts the unmarked samples individually according to the model they are learning. If the unmarked samples combination with the best classification results, then the predictive accuracy should be higher than the predictions of the subclassifiers. However, when the difference in the subclassifiers is greater, a lower confidence level is predicted. When this phenomenon occurs, multiclassifier combinations cannot improve the accuracy.
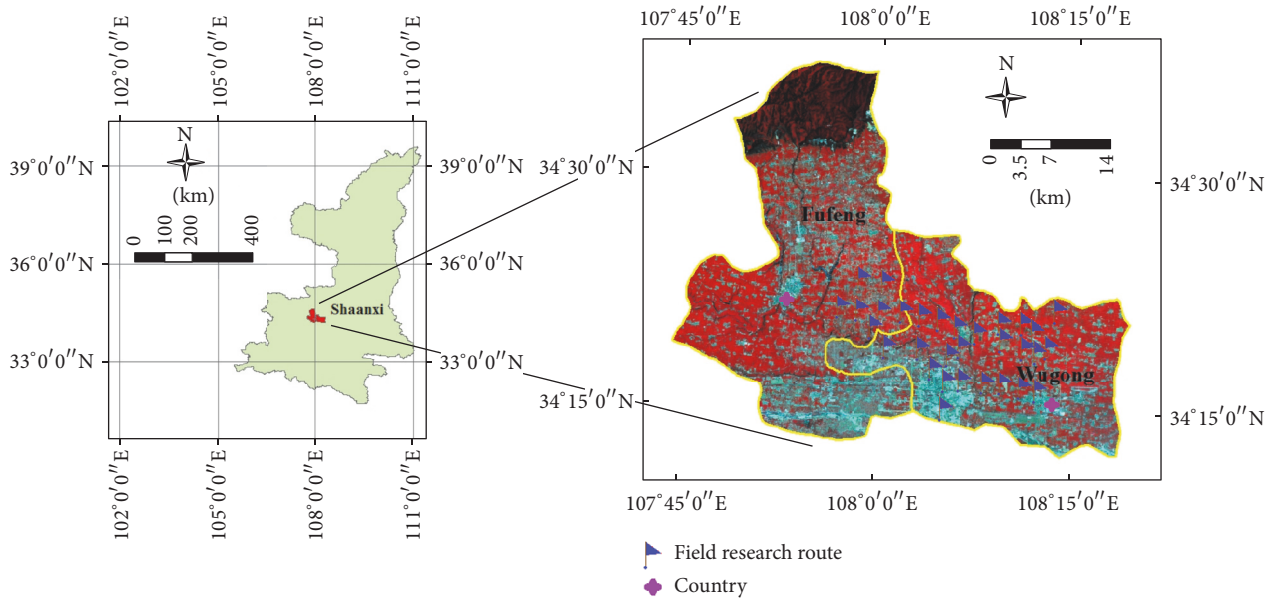
FIGURE 1: Location and the field research route of the study area in China. The magnified map is a false-color mosaic (red-green-blue (RGB): Bands 4, 3, and 2, resp.) of HJ-1 CCD data.

The normalized difference vegetation index (NDVI) is a critical parameter for identifying vegetation, and it has an obvious correlation with vegetation cover [19]. Because temporal variation corresponds to vegetation change and growth, areas that have the same vegetation exhibit similar curves. Therefore, the long-term sequence of NDVI information derived from long-term remote-sensing images has led to NDVI time series of remote-sensing data becoming a crucial source of information on land cover classification [20–22]. Compared with the traditional classification approach with different intervals from NDVI time series, the use of daily NDVI time series remote-sensing data classification often improves the classification accuracy because it derives more phenological features that have a statistically significant effect on improving land cover classification accuracy [23, 24]. However, daily NDVI time series remote sensing is prone to data loss, and unequal intervals cannot fully reveal the change of land-cycle vegetation index [25]. Moreover, this technique suffers from reduced land classification accuracy during bad weather and when the satellite return cycle is not reached [26]. These are crucial constraints on land classification based on NDVI time sequences [27]. Daily NDVI time sequences have higher dimensions that may cause the process of feature selection to be very cumbersome and result in particularly large calculations. This study was to employ HJ-1 data to develop a process flow to construct a daily NDVI time series for land cover classification.

The aim of the present study was to employ HJ-1 data for land cover classification based on daily NDVI time series and multiclassifier combination. The objectives of this study were to (1) classify land cover from daily NDVI time series with different classifiers; (2) propose a method of land cover information extraction with statistical features based on daily NDVI time series; (3) classify land cover from daily NDVI time series with a multiclassifier combination to improve the classification accuracy; (4) propose an improved method of multiclassifier combination to improve the classification accuracy when the difference in subclassifiers is particularly large.

2. Study Area and Remote-Sensing Data

2.1. Study Area. The Guanzhong Plain area in Shaanxi Province, China, is a key production base for grain, oil, fruit, and vegetables. Land management planning with a timely grasp of the land cover situation is of great significance in the area. In this study, the counties of Wugong and Fufeng were selected from the Guanzhong Plain area and examined (Figure 1). Wugong ($108°01'$–$108°19'$E, $34°12'$–$34°26'$N) and Fufeng ($107°45'$–$108°4'$E, $34°12'$–$34°37'$N) cover an area of $1210.2 \, km^2$. The study area has a continental semihumid monsoon climate with an average annual temperature of approximately $12.7°C$; its average precipitation is 600 mm, and the region is characterized by rich sunshine, and flat, fertile land. It is a typical drought-prone region of northern China [28, 29] and is dominated by woodland and cultivated land. Apples and kiwis are the main woodland produce, and winter wheat and corn are the main cultivated land crops. This study considers the land with winter wheat and corn as cultivated land.

2.2. Samples Selection. The selection of different categories of samples plays a key role in establishing classification information and classification rules. With the Current Land Use Classification for National Standard of the People's Republic of China (GB/T21010-2007) as the base reference of land categories and considering the field research, visual interpretation using high-resolution images and dominant ecosystems [30], ten land use categories were interpreted

TABLE 1: Samples table in study area.

Sample category	C1	C2	C3	C4	C5	C6	C7	C8	C9	C10
Training sample	168	157	194	168	192	281	167	185	212	163
Testing sample	396	368	366	386	388	366	375	366	436	367

Note. C1: woodland; C2: kiwi orchard; C3: bare rocky gravel; C4: river canal; C5: beach; C6: sandy ground; C7: rural residential area; C8: cultivated land; C9: town; C10: apple orchard.

TABLE 2: HJ-1 CCD satellite data characteristics.

Spatial resolution (m)	Spectral bands (μm)	Swath (km)	Temporal resolution (days)
30	B1 0.43–0.52; B2 0.52–0.60; B3 0.63–0.69; B4 0.76–0.90;	More than 700	2

including cultivated land, woodland, river canal, beach, rural residential, town, bare rocky gravel, sandy ground, apple orchard, and kiwi orchard. Considering the actual land use characteristics, we did not divide cultivated land into sublevel types but divided orchard into sublevel types (apple orchard and kiwi orchard) [31]. Given the coarse image resolution and fragmented distributions of bare rocky gravel and bare land, we merged bare rocky gravel and bare land into bare rocky gravel [32].

This study selected training and testing samples through field research and defined region of interest (ROI) files by ENVI 5.0 software for different land cover categories using ground true data [33]. To ensure the accuracy of the samples, the training and testing samples were selected and validated as follows: (1) the sample type was determined through the first field research and an analysis of land use, (2) the sample type and regions were confirmed further with HJ-1/CCD images and high-resolution images from Google Earth, and (3) the sample types and region accuracy were further confirmed through a second field survey with the same research route. The field research of this study includes category type, latitude and longitude, and then we selected the effective samples in the remote sensing data after filed research. The field research route and sample table are shown in Figure 1 and Table 1. The chosen samples were evenly distributed in the study area.

2.3. Remote-Sensing Data. HJ-1 satellite data were retrieved from the China Centre for Resources Satellite Data and Application (http://www.cresda.com/), which is the most appropriate optical data source with combined temporal and spatial resolution for remote-sensing monitoring [34]. It is characterized by a large volume, high spatial resolution with a 30 m pixel resolution at the nadir angle, and high time resolution with a 2-day repeat cycle. The main characteristics of HJ-1 CCD satellite data are shown in Table 2.

The study selected 55 images in total for analysis. The therein 51 main remote-sensing images were HJ-1 CCD images captured from June 2015 to May 2016; cloud cover in the images was less than 10%. Because of the vegetation indices of the HJ-1 CCD and Landsat images exhibiting a significantly positive linear correlation [35], 4 Landsat images were supplemented during the serious loss of growth cycle image stage.

3. Materials and Methods

3.1. Data Preprocessing. Conventional preprocessing procedures can be used for HJ-1 CCD images. Images were projected into UTM with WGS 84 ellipsoid. The metadata files attached to these images contain detailed information on image status. HJ-1 data preprocessing procedures include radiation correction, geometric correction, atmospheric correction, and subset selection with the study area [36, 37]. The image DN value is transformed into a radiation brightness value by obtaining the radiation calibration coefficients. In this study, FLAASH atmospheric correction was performed using ENVI 5.0 [36], and then the research area was cut. The final geometric correction of the HJ-1 CCD image processing used the Landsat Thematic Mapper image as a reference, 60 ground control points, and a correction error control of 0.5 pixels [38].

The NDVI was calculated using the red and near-infrared data from HJ-1 CCD data. The NDVI time series data set for the study area was obtained by superimposing the NDVI images according to their acquisition time [39]:

$$\text{NDVI} = \frac{\rho_{\text{NIR}} - \rho_{\text{R}}}{\rho_{\text{NIR}} + \rho_{\text{R}}}, \tag{1}$$

where ρ_{NIR} and ρ_{R} are the surface reflectance of the near-infrared and red band, respectively.

Because the NDVI time series of the acquired HJ-CCD images are unequally spaced, many filtering methods based on the signal frequency are not applicable. In this study, the Savitzky–Golay (S-G) filtering [40, 41] algorithm was applied. S-G filtering is based on using the least squares convolution method to smooth and calculate the function of the adjacent value, and the local adaptive fitting can handle signals with unequal intervals; the basic formula of the method is as shown in

$$G_j^* = \frac{\sum_{i=-m}^{i=m} C_i G_{j+1}}{N}, \tag{2}$$

where G represents the original NDVI time series of values, G^* represents the value after smooth, m is a positive integer, $2m + 1$ represents the size of the sliding window, N is the number of convolution, the value is equal to the sliding window size, C_i can be calculated by the formula proposed

by Madden [42], and j is the coefficient of the original NDVI array.

This study realized the filtering and daily interpolation based on the spatial time series of image pixels, which is based on the time series reconstruction system developed by Pan et al. [25]. The system uses linear interpolation technology to achieve the function of interpolation. The basic principle of the system relational expression is as shown in [25]

$$\text{NDVI} = \text{NDVI}_0 + (\text{NDVI}_1 - \text{NDVI}_0)$$
$$* \frac{\text{DAY} - \text{DAY}_0}{\text{DAY}_1 - \text{DAY}_0}, \tag{3}$$

where NDVI represents the date to be interpolated and NDVI_1 and NDVI_0 represent the acquired image sequence.

3.2. Quick Unbiased and Efficient Statistical Tree.
Quick Unbiased and Efficient Statistical Tree (QUEST) is a decision tree algorithm proposed by Loh and Shih in 1997 and it has since been continuously improved [43]. QUEST is a type of decision tree classification approach that classifies according to classification rules based on expert experience, simple mathematical statistics, and induction methods; it is widely used for land cover classification [44]. The QUEST classifier used in this study relied on the RuleGen v.1.02 software in IDL/ENVI language. RuleGen analyzes train samples to generate ENVI decision tree project files, and then the rule is applied to the entire remote-sensing data.

3.3. Spectral Angle Mapper.
SAM is a technique for hyperspectral image analysis proposed by Kruse et al. [45], which is a standardized, fast, and simple method for calculating spectral similarities between an investigated object and a reference object. The smaller the calculated angle is, the more similar the two spectra are [46]. Therefore, an object's spectrum is assigned to the class that has the smallest angle value regarding the specific reference spectrum.

In this study, we first obtain the spectral curve of the training samples and take them as a reference spectral curve for train samples. Last we extracted the land cover information through SAM based on reference spectral curve for each sample.

3.4. Other Classification Methods.
Remote-sensing image classification is based on spectral characteristics and involves the extraction of the background of an image from a target image. According to whether there is a priori knowledge of the spectrum, the target detection algorithm can be divided into two categories: supervised and unsupervised. This study mainly used K-means [47] unsupervised classification, Mahalanobis distance [48], minimum distance [49], and SVM [50] for supervision classification. Mahalanobis distance, minimum distance, and SVM were applied to explore all the input features according to given training samples. K-means classification is the classification of patterns derived from remote-sensing data into classes and does not require training.

SVM classifier for land cover classification is applied using ENVI 5.0 remote-sensing software in this study, and the selection of kernel functions in this study is default parameters in ENVI 5.0.

3.5. Classification Method Based on the Statistical Characteristics of a Time Series.
Time series data reflect the characteristics of attribute values in temporal and spatial order. Using time series data mining can yield useful information related to time in data and realize the extraction of knowledge.

This study involved land information extraction research based on the daily NDVI time series. Time series classification problems have been widely addressed in the field of time series data mining, in which they are treated as a branch of sequence classification problems [51]. Because the dimension of the time series feature space is very large, the process of feature selection in time series classification is very cumbersome and the calculation is very large. A feature refers to an object's polygon attribute information including the spectrum, texture, shape, spatial relations, topology, and other information. Data dimension reduction and feature representation are the key technologies and methods for solving the large dimension problem of time series. In this paper, we propose a method of dimensionality reduction and feature representation of time series data to classify time series according to their statistical features from daily NDVI time series. This can facilitate the feature selection process and lessen the computation involved in the classification process.

Based on the statistical characteristics of different samples, the mean, standard deviation, variance, skewness, kurtosis, and mean absolute deviation of daily NDVI time series were selected as the sample characteristics. Because of the existence of bimodality in cultivated land, this study divided the time series into two stages: the growth stage of corn and the growth stage of winter wheat. The statistical characteristics of NDVI time series were calculated using ENVI5.0, and the statistical characteristics of different sample types were extracted as shown in Figure 2. A range of variations were found in the statistical characteristics between different samples. The mean, skewness, and kurtosis differed markedly among sample types, and the standard deviation, variance, and mean absolute deviation were relatively the same. Only the difference between the samples was marked; however, a greater level of distinction between them could be achieved. Therefore, three statistical characteristics (i.e., the mean, skewness, and kurtosis) were selected as the daily NDVI time series characteristics for distinguishing between samples. An SVM classifier was used to achieve the classification results using three statistical features based on the daily NDVI time series.

3.6. Multiclassifier Combination.
Voting methods are among the most commonly used multiclassifier combination methods [52–54] and are used to determine whether the members of classifier output results differ. The category with the most voting rules is classified as the category of the class that consistently distinguishes the most classifiers. When multiple categories have an identical vote number, one of them tends
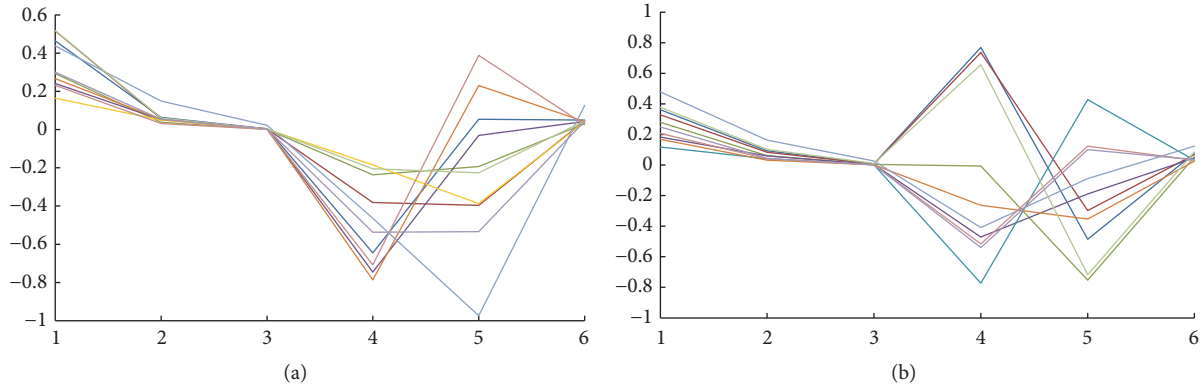
FIGURE 2: Statistical information of different samples. 1: mean; 2: standard deviation; 3: variance; 4: skewness; 5: kurtosis; 6: mean absolute deviation. (a) Statistical information of various samples during corn growth. (b) Statistical information of various samples during winter wheat growth.

to be randomly selected as the final result. This study applied a weighted voting method. That classification ability of accurate classifiers should be assigned a higher probability value, and poor classification classifiers assigned a lower probability value.

3.7. Improved Multiclassification Combination Method. When there is a greater difference between the subclassifiers, the confidence level of prediction is lower. For example, the classification accuracy of one classifier is far superior to other classifiers, which leads to the classification accuracy of the multiclassifier combination results being lower than that of the optimum classifier. Therefore, an improved classifier combination method is proposed, in which the following algorithm steps are used:

(1) The first and second steps are identical to those in the voting method.

(2) The classification probability images are compared with the same classifier class and the different class optimal classification probability images are thus obtained. The different class classification probabilities are compared for the unknown pixel *X*, and the category corresponding to the maximum value of pixel *X* is selected the final category label.

Multiclassifier combination methods were not reclassified, they were just all the pixel reclassified based on the remote-sensing data, different type and different single classifiers have different probability and we sum the different type probability with different single classifiers, and last the maximum probability of the sample is the result of the classification.

3.8. Accuracy Evaluation of Classification Results. Confusion matrices are the most commonly used method for evaluating the classification accuracy of remote-sensing images [55]. They are mainly used to compare the classification results with real information from the surface. The accuracy of the classification results can be displayed in a confusion
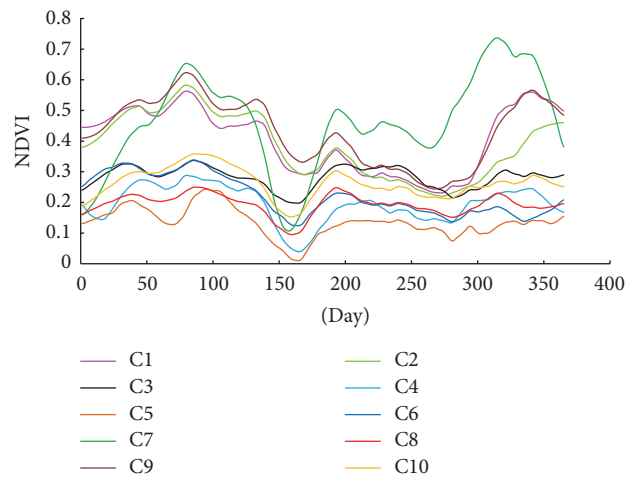

FIGURE 3: Curve of NDVI time series. C1: woodland; C2: kiwi orchard; C3: bare rocky gravel; C4: river canal; C5: beach; C6: sandy ground; C7: cultivated land; C8: town; C9: apple orchard; C10: rural residential area; the corresponding number of days for the curves abscissa is from June 11, 2015, to June 10, 2016.

matrix. A confusion matrix has the following evaluation indices: overall accuracy, Kappa coefficient, prod accuracy, omission, user accuracy, and commission. This study selected overall accuracy, Kappa coefficient, prod accuracy, and user accuracy as the evaluation indices of remote-sensing image classification accuracy.

4. Results

4.1. Daily NDVI Time Series of Sample Category. The daily NDVI time series curves of the sample categories showed a distinct difference after smoothing and spatial interpolation (Figure 3). In Figure 3, the daily NDVI time series after pretreatment are enhanced in the time dimension and reflect the subtle changes in NDVI of the different sample categories during the year. The NDVI time series of the river canal and beach have lower troughs than the other time series.

TABLE 3: The classification results based on time series statistics and SVM classifier.

Index	C1	C2	C3	C4	C5	C6	C7	C8	C9	C10
Prod accuracy (%)	65.15	73.91	69.95	61.40	88.66	84.7	82.93	100.00	68.81	81.74
User accuracy (%)	78.90	76.62	73.35	83.45	78.90	69.98	66.45	100.00	77.12	75.57
Overall accuracy	77.45%									
Kappa coefficient	0.7495									

Note. C1: woodland; C2: kiwi orchard; C3: bare rocky gravel; C4: river canal; C5: beach; C6: sandy land; C7: rural residential area; C8: cultivated land; C9: town; C10: apple orchard.

TABLE 4: Classification results based on QUEST (SAM).

Index	C1	C2	C3	C4	C5	C6	C7	C8	C9	C10
Prod accuracy (%)	79.55 (38.13)	76.36 (71.47)	80.87 (66.67)	95.85 (88.60)	91.24 (75.68)	92.08 (75.68)	89.33 (84.00)	98.63 (100.00)	81.65 (86.24)	88.56 (51.23)
User accuracy (%)	85.83 (52.80)	72.80 (62.03)	93.97 (94.94)	94.87 (91.44)	90.08 (100.00)	88.92 (75.68)	80.53 (63.13)	100.00 (98.39)	74.48 (76.11)	98.78 (40.96)
Overall accuracy	87.31% (73.52%)									
Kappa coefficient	0.8589 (0.7057)									

Note. Parameters in brackets are the classification results of SAM and the parameters outside brackets are the classification results of QUEST; C1: woodland; C2: kiwi orchard; C3: bare rocky gravel; C4: river canal; C5: beach; C6: sandy ground; C7: rural residential area; C8: cultivated land; C9: town; C10: apple orchard.

The daily NDVI time series curve of the cultivated land has two conspicuous growth peaks, whereas the woodland, apple orchards, and kiwi orchards have one growth peak. The maximum value, minimum value, and change rate of the NDVI differ among the different sample categories. The growth peak of the NDVI in the woodland is less than that in the other areas, and the NDVI curves in the sample categories of nonvegetation are unstable, with the exception of sample categories involving water. All the information revealing differences between the different sample categories is critical for their classification.

4.2. Classification Results Based on Time Series Statistics. An SVM classifier was used to classify the images of the mean, peak, and skewness of daily NDVI time series, the final results of which were verified using a confusion matrix. The classification results are shown in Table 3.

The overall accuracy of the classification results based on NDVI time series statistics is 77.45% and the Kappa coefficient is 0.7495, indicating a high degree of consistency. The results of the classification of cultivated land were the most accurate, with the user accuracy reaching 100% and the prod accuracy being 100%. The classification map is shown in Figure 4.

4.3. Classification Results Based on QUEST and SAM. QUEST was used to examine all the train samples features and automatically built tree rules based on the given training samples. SAM was used to examine all the object reference spectrums according to the given training samples. The daily NDVI time series based on the tree rules and object reference spectrums were then classified. The final classification results were verified using a confusion matrix and are shown in Table 4.

The overall accuracy of the classification results obtained by applying SAM to the daily NDVI time series is 73.52%

and the Kappa coefficient is 0.7057, indicating a high degree of consistency. The overall accuracy of classification results yielded by applying QUEST to the daily NDVI time series is 87.31% and the Kappa coefficient is 0.8589, indicating almost complete consistency. The classification map is shown in Figure 4.

4.4. Other Single Classifier Classification Results. Based on daily NDVI time series, we employed both unsupervised and supervised classification methods to classify the time series. The final results were verified using a confusion matrix and are shown in Table 5.

The overall accuracy of the classification results based on the daily NDVI time series with Mahalanobis distances and SVM are 97.72% and 94.23%, and the Kappa coefficients are 0.9746 and 0.9359, respectively, indicating almost complete consistency. This approach can more effectively realize the land cover classification and extraction of land resources information for daily NDVI time series. The overall accuracy of NDVI time series with minimum distance classification results is 68.12% and the Kappa coefficient is 0.6455, indicating a high degree of consistency. This approach can also be used to realize land classification and land resource information extraction. However, the effectiveness of the K-means unsupervised classifier was low, with overall accuracy and Kappa coefficient of only 20.69% and 0.1175, respectively, indicating that this method cannot be used for land classification or land resource information extraction. K-means classification is processed based on the similarity calculation obtained from the average values of objects in different categories. However in present study, the difference between spectral information of categories is unequal. And under this circumstance, the similar spectral information is classified into one category, and some mixed-pixel is misinterpreted into one category. In the present study prod accuracy and user accuracy values are 0 for kiwi orchard, bare rocky
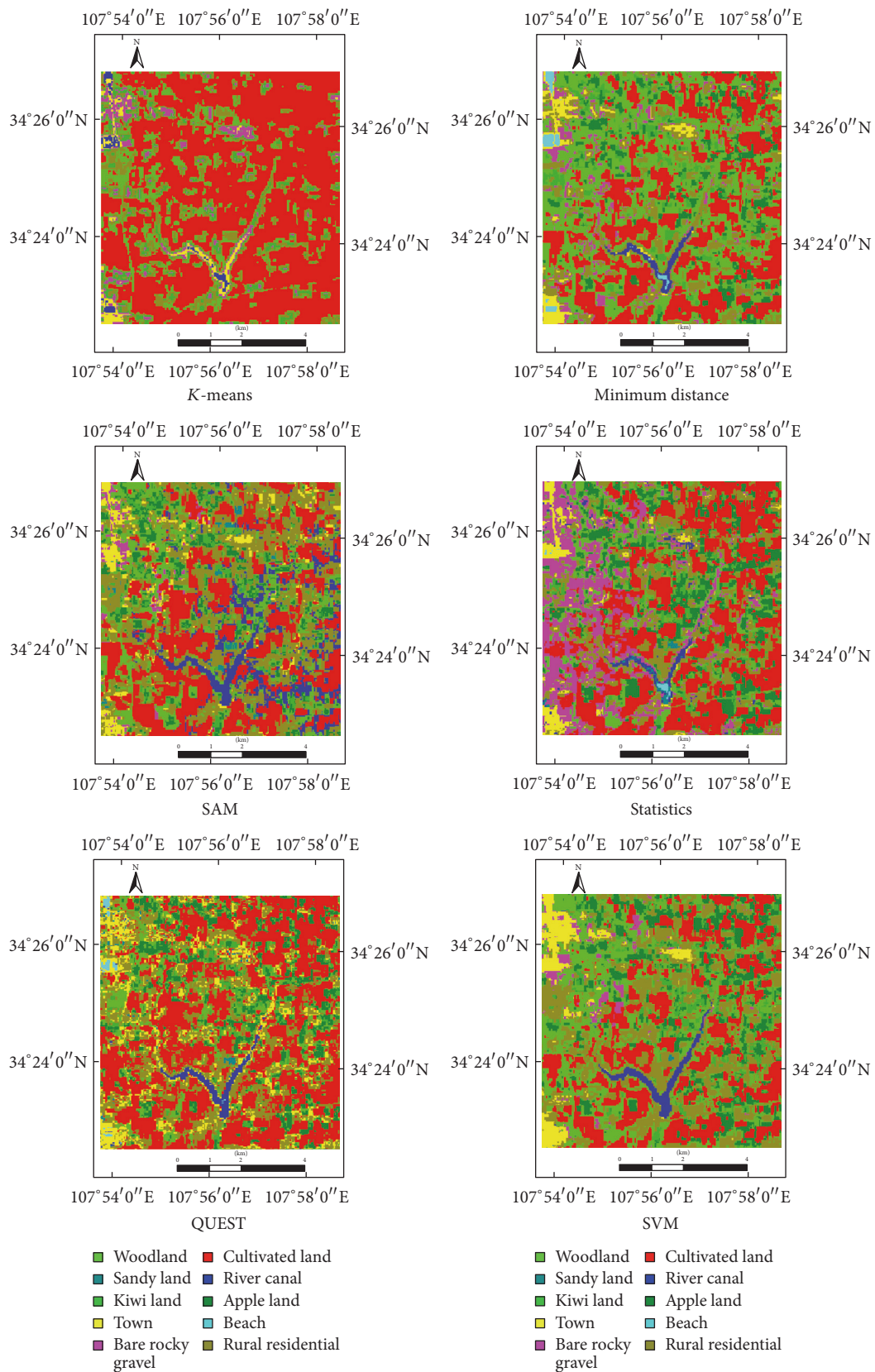
FIGURE 4: The classification maps of daily NDVI time series with different classifiers.

TABLE 5: Classification results of other single classifiers.

Index	K-means		Mahalanobis distance		Minimum distance		SVM	
	PA (%)	UA (%)	PA (%)	UA (%)	PA (%)	UA (%)	PA (%)	UA (%)
C1	22.98	44.61	92.17	99.18	61.11	72.24	93.18	93.42
C2	0	0	99.46	94.82	74.18	63.49	77.72	85.37
C3	0	0	98.09	99.72	31.97	75.48	93.44	99.71
C4	24.87	20.17	99.22	100	76.42	87.54	99.48	96.73
C5	0.26	0.21	97.16	99.74	88.4	56.05	95.88	99.47
C6	3.01	7.33	99.18	95.03	71.04	96.3	93.72	98.56
C7	28.53	36.15	94.4	96.99	69.87	59.68	98.4	80.92
C8	100	27.83	100	99.46	100	99.46	100	100
C9	26.83	16.88	99.08	97.3	42.66	39.24	98.62	95.13
C10	0	0	98.64	95.26	69.21	64.47	90.74	95.69
Overall accuracy	20.69%		97.72%		68.12%		94.23%	
Kappa coefficient	0.1175		0.9746		0.6455		0.9359	

Note. PA: prod accuracy; UA: user accuracy; C1: woodland; C2: kiwi orchard; C3: bare rocky gravel; C4: river canal; C5: beach; C6: sandy ground; C7: rural residential area; C8: cultivated land; C9: town; C10: apple orchard.

TABLE 6: Classification results of multiclassifier combination.

Index	SAM + minimum distance + statistics		SAM + SVM + QUEST	
	PA (%)	UA (%)	PA (%)	UA (%)
C1	69.19 (65.15)	75.90 (79.63)	95.20 (92.68)	93.09 (95.32)
C2	74.18 (73.91)	67.24 (76.62)	77.72 (77.72)	82.90 (85.37)
C3	77.87 (70.22)	87.42 (88.93)	91.53 (93.44)	98.82 (99.71)
C4	86.79 (90.93)	87.24 (90.70)	99.48 (99.48)	96.24 (96.73)
C5	88.92 (84.28)	81.18 (86.51)	95.10 (95.36)	99.46 (99.46)
C6	78.14 (73.50)	92.56 (91.81)	93.40 (93.72)	98.30 (98.56)
C7	84.80 (90.93)	73.61 (59.82)	96.50 (98.40)	79.90 (80.92)
C8	100.00 (100.00)	99.19 (100.00)	100.00 (99.45)	99.73 (100.00)
C9	69.21 (81.19)	75.91 (77.80)	98.17 (98.62)	94.07 (94.71)
C10	68.12 (81.74)	70.17 (75.57)	87.47 (92.92)	96.69 (95.25)
Overall accuracy	80.49% (81.15%)		93.60% (94.28%)	
Kc	0.7832 (0.7905)		0.9289 (0.9365)	

Note. The columns show the classification results of the original multiclassifier with those for the improved multiclassifier combination shown in parentheses; PA: prod accuracy; UA: user accuracy; Kc: Kappa coefficient; C1: woodland; C2: kiwi orchard; C3: bare rocky gravel; C4: river canal; C5: beach; C6: sandy ground; C7: rural residential area; C8: cultivated land; C9: town; C10: apple orchard.

gravel, and apple orchard classification because of similar curves classified into one class. And this is further confirmed that this method cannot be used for land classification with daily NDVI time series. The classification map is depicted in Figure 4.

The process of calculating the Mahalanobis distance requires the overall sample number to be higher than the dimension number of the sample; otherwise, the inverse matrix of the overall sample covariance matrix cannot be obtained [56, 57]. Therefore, in this study the classification training samples could not be applied because the overall sample number was lower than the size of the scale, and certified samples were selected for classification and verification. For high-dimensional sequence classification, it is not recommended to use the Mahalanobis distance classifier because this requires a high number of samples, which leads to an increase in the difficulty of classifying smaller area types; consequently, feature classification cannot be achieved for such area types.

4.5. Classification Results of Multiclassifier Combination.
Based on the daily NDVI time series multiclassifier combination method, two types of combinations were applied: SAM, minimum distance, and statistical characteristics; and SAM, SVM, and QUEST. The final classification results were verified using a confusion matrix and shown in Table 6. Prod accuracy and user accuracy represents the degree of consistency between the actual classification and the reference classification and the degree of consistency between the actual classification number and the classification number, respectively.

The classification results based on the original multiclassifier combination indicate that the overall accuracy of the three-classifier combination with SAM, minimum
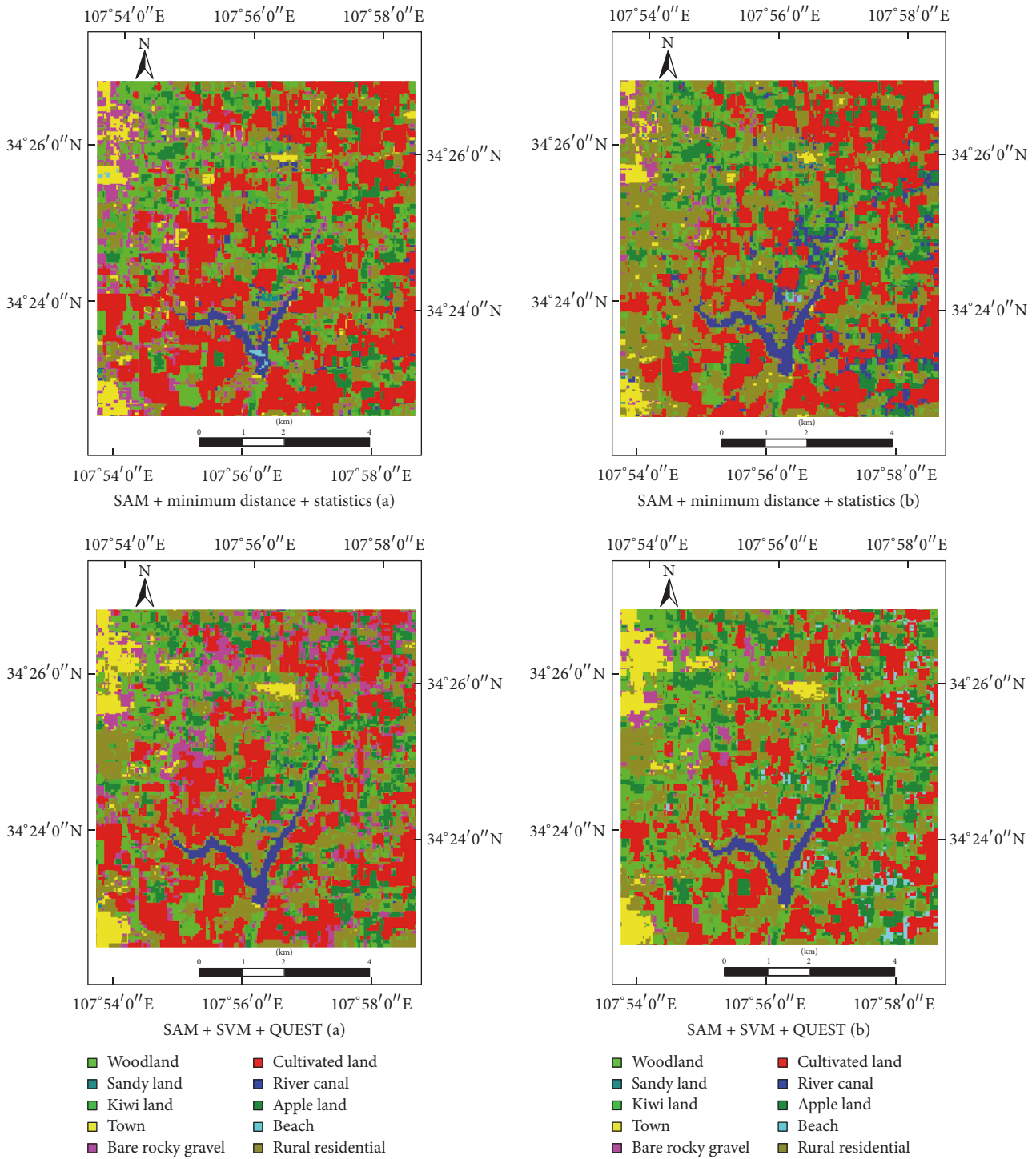
FIGURE 5: Classification maps of daily NDVI time series with different multiclassifier combination.

distance, and statistical characteristics was 80.49% and the Kappa coefficient was 0.7832; those of the other three-classifier combination were 93.60% and 0.9289, respectively. The classification results yielded by the improved multiclassifier combination indicated that the overall accuracy of the

three-classifier combination of SAM, minimum distance, and statistical characteristics was 81.15% and the Kappa coefficient was 0.7905. The other three-classifier combination had an overall accuracy of 94.28% and a Kappa coefficient of 0.9365. The classification map is shown in Figure 5.

5. Discussion

(1) The daily NDVI time series can be constructed through S-G filtering and spatial interpolation according to the resource satellite data. It contains subtle information in the temporal and spatial dimensions, thereby contributing more information to the extraction of land resource information. However, the large spatial dimension of the series may cause the classification process to be cumbersome and computationally demanding. Spectral feature extraction can be used to reduce the dimensions and obtain information with as high dimension data as possible. Gasmi et al. [58] used principal component analysis to reduce the dimensions of the 9 ASTER bands, yielding results that correlated well with a reference geological map. In the present study, because of the large spatial dimension of the daily NDVI time series, the statistical characteristics were selected to realize their classification. The analysis of the classification results indicates that the daily NDVI time series can be classified based on images of mean, kurtosis, and skewness. The overall accuracy is 77.45% and the Kappa coefficient is 0.7495, indicating a high degree of consistency (Table 3 and Figure 4). The classification results indicate that the method is effective. Applying classification methods that are based on the statistical characteristics of daily NDVI time series solves the problem of the spatial dimension of daily NDVI time series being large and cumbersome to process. This study proposes a new method for classifying daily NDVI time series and other large dimension classifications.

(2) 6 single classifiers—namely, QUEST, SAM, minimum distance, Mahalanobis distance, SVM, and K-means—were applied to daily NDVI time series. Ouzemou et al. (2015) applied SVM and SAM methods to classify principal crops using NDVI time series of 10 periods and reported overall accuracies of 85.27% and 57.17%, respectively [59]. The results of the present study demonstrate that a single classifier based on SVM and the Mahalanobis distance achieves a high level of accuracy in extracting land resource information from daily NDVI time series data, with a Kappa coefficient of >0.90 (Table 5). However, because of its mechanism, a single classifier based on the Mahalanobis distance is unsuitable for extracting information from daily NDVI time series. Based on the single classifiers QUEST, SAM, and minimum distance, land resource information can be extracted using daily NDVI time series, with Kappa coefficients of 0.8589, 0.7057, and 0.6812, respectively, indicating a high degree of consistency (Tables 4 and 5; Figure 4). This indicates that QUEST, SAM, and minimum distance are suitable for extracting land resource information from daily NDVI time series and other time series. The study area has more object categories and a large number of mixed pixels. The NDVI curves of the various sample categories differ markedly, with some curves exhibiting little difference and others exhibiting large differences. K-means is unsuitable for daily NDVI time series with mixed pixels and high variation, because it is an unsupervised classification algorithm based on distance. The Kappa coefficient of the K-means single classifier in the daily NDVI time series is 0.1175 (Table 5), which indicates it cannot satisfy the requirement of land resource information extraction. This further indicates that K-means is unsuitable for extracting information from daily NDVI time series. The classification maps of different classifiers reveal that different classifiers have different accuracy in different sample classes. The classification map indicates that the SVM yielded the optimal map, followed by the QUEST and SAM results maps. The worst classification map is that produced using the K-means classifier. The results of 6 single classifiers for daily NDVI time series classification indicate that SVM classifiers are the optimal classifier for daily NDVI time series classification and that QUEST, SAM, and minimum distance are suitable for extracting land resource information from daily NDVI time series, whereas K-means is unsuitable.

(3) The daily NDVI time series was processed based on the multiclassifier combination. The results indicate that the overall classification accuracy of the three-classifier combination based on SAM, minimum distance, and statistical features was 80.49% and the Kappa coefficient was 0.7832 (Table 6), which is more favorable than the classification results of each of the three types of classifiers alone. This demonstrates that multiclassifier combination can be effectively applied to weak classifier combinations. Using the SAM, QUEST, and SVM three-classifier combination attained an overall classification accuracy of 93.60% and Kappa coefficient of 0.9289 (Table 6), indicating that despite its classification ability being superior to that of the SAM and QUEST single classifier results, it is lower than the SVM classification results. When the difference in the subclassifiers is greater, the confidence level of prediction is lower and the classification results are worse than those of the subclassifiers. This indicates that the multiclassifier combination is less effective than applying different precision classifiers.

The improved multiclassifier combination results indicate that the overall classification accuracy of the three-classifier combination of SAM, minimum distance, and statistical features was 81.15% and the Kappa coefficient was 0.7905 (Table 6). The overall classification accuracy of the three-classifier combination of SAM, QUEST, and SVM was 94.28% and the Kappa coefficient was 0.9365 (Table 6). Compared with the original multiclassifier combination algorithm, the improved multiclassifier combination attained accuracy that was consistent with the overall accuracy and Kappa coefficient of the three-classifier combination of SAM, minimum distance, and statistical characteristics. The classification map indicates that the results are consistent and have high accuracy compared to the subclassifiers alone. Comparing two multiclassifier combination algorithms revealed that the improved multiclassifier combination has higher accuracy than the original algorithm and the subclassifiers; however, the original multiclassifier combination is less accurate than the optimal subclassifiers, which means it is unsuitable for subclassifiers with greater differences. The results indicate that the improved multiclassifier combination is superior to the original multiclassifier combination algorithm and that all the combination results are better than those of the subclassifiers. In particular, the combination effect is more effective for the classification of subclassifiers with greater differences.

6. Conclusions

In this study, the HJ-CCD satellite was used as a data source to construct NDVI time series by S-G filtering and spatial interpolation.

A method of dimensionality reduction using the statistical features of daily NDVI time series was proposed. The results show that the overall accuracy of the statistical images results based on daily NDVI time series is 77.45%, which demonstrates that this method can be applied for extracting land resource information.

We developed a new method for daily NDVI time series classification based on multiclassifier combination. Three-classifier combinations with greater differences are not useful to improve classification results. This study proposes an improved multiclassifier combination method. The proposed improved multiclassifier combination was demonstrated to provide enhanced performance in different single classifier combinations, especially for subclassifiers with greater differences.

Conflicts of Interest

The authors declare that there are no conflicts of interest regarding the publication of this paper.

Acknowledgments

References

[1] S. T. Jarnagin, "Regional and global patterns of population, land use, and land cover change: an overview of stressors and impacts," *GIScience & Remote Sensing*, vol. 41, no. 3, pp. 207–227, 2004.

[2] E. Yeshaneh, W. Wagner, M. Exner-Kittridge, D. Legesse, and G. Blöschl, "Identifying land use/cover dynamics in the koga catchment, Ethiopia, from multi-scale data, and implications for environmental change," *ISPRS International Journal of Geo-Information*, vol. 2, no. 2, pp. 302–323, 2013.

[3] N. Clerici, M. L. Paracchini, and J. Maes, "Land-cover change dynamics and insights into ecosystem services in European stream riparian zones," *Ecohydrology & Hydrobiology*, vol. 14, no. 2, pp. 107–120, 2014.

[4] W. Wahyunto, W. Supriatna, and F. Agus, "Land use change and recommendation for sustainable development of peatland for agriculture: case study at Kubu Raya and Pontianak Districts, West Kalimantan," *Indonesian Journal of Agricultural Science*, vol. 11, no. 1, p. 32, 2010.

[5] C. Xiuwan, "Using remote sensing and GIS to analyse land cover change and its impacts on regional sustainable development," *International Journal of Remote Sensing*, vol. 23, no. 1, pp. 107–124, 2002.

[6] C. Prakasam, "Land use and land cover change detection through remote sensing approach: a case study of kodaikanal taluk, tamil nadu," *International Journal of Geomatics & Geosciences*, pp. 150–158, 2010.

[7] Y. Setiawan, E. Rustiadi, K. Yoshino, Liyantono, and H. Effendi, "Assessing the seasonal dynamics of the Java's paddy field using MODIS Satellite Images," *ISPRS International Journal of Geo-Information*, vol. 3, no. 1, pp. 110–129, 2014.

[8] A. Reyes, M. Solla, and H. Lorenzo, "Comparison of different object-based classifications in LandsatTM images for the analysis of heterogeneous landscapes," *Measurement*, vol. 97, pp. 29–37, 2017.

[9] M. T. Rahman, "Detection of land use/land cover changes and urban sprawl in Al-Khobar, Saudi Arabia: an analysis of multi-temporal remote sensing data," *ISPRS International Journal of Geo-Information*, vol. 5, no. 2, article 15, 2016.

[10] T. L. Grobler, E. R. Ackermann, J. C. Olivier, A. J. Van Zyl, and W. Kleynhans, "Land-cover separability analysis of MODIS time-series data using a combined simple harmonic oscillator and a mean reverting stochastic process," *IEEE Journal of Selected Topics in Applied Earth Observations and Remote Sensing*, vol. 5, no. 3, pp. 857–866, 2012.

[11] Z. Xie, R. Shi, L. Zhu, S. Peng, and X. Chen, "Comparison of pixel-based and object-oriented land cover change detection methods," in *Proceedings of the 23rd International Archives of the Photogrammetry, Remote Sensing and Spatial Information Sciences Congress (ISPRS '16)*, pp. 579–583, Prague, Czech Republic, July 2016.

[12] P. Kumar, D. K. Gupta, V. N. Mishra, and R. Prasad, "Comparison of support vector machine, artificial neural network, and spectral angle mapper algorithms for crop classification using LISS IV data," *International Journal of Remote Sensing*, vol. 36, no. 6, pp. 1604–1617, 2015.

[13] Y. Megahed, P. Cabral, J. Silva, and M. Caetano, "Land cover mapping analysis and urban growth modelling using remote sensing techniques in greater Cairo region—Egypt," *ISPRS International Journal of Geo-Information*, vol. 4, no. 3, pp. 1750–1769, 2015.

[14] B. Ahmed and M. A. A. Noman, "Land cover classification for satellite images based on normalization technique and Artificial Neural Network," in *Proceedings of the 1st International Conference on Computer and Information Engineering (ICCIE '15)*, pp. 138–141, Rajshahi, Bangladesh, November 2015.

[15] H. Luo, L. Li, H. Zhu, X. Kuai, Z. Zhang, and Y. Liu, "Land cover extraction from high resolution ZY-3 satellite imagery using ontology-based method," *ISPRS International Journal of Geo-Information*, vol. 5, no. 3, article 31, 2016.

[16] G. Giacinto and F. Roli, "Ensembles of neural networks for soft classification of remote sensing images," in *Proceedings of the European Symposium on Intelligent Techniques*, pp. 166–170, Bari, Italy, March 1997.

[17] D. Cao, Q. Yin, and P. Guo, "Multi-source remote sensing classification based on Mallat fusion and residual error feature selection," *Journal of Digital Information Management*, vol. 5, no. 3, pp. 130–137, 2007.

[18] M. Habibi, M. R. Sahebi, Y. Maghsoudi, and S. Ghayourmanesh, "Classification of polarimetric SAR data based on object-based multiple classifiers for Urban Land-Cover," *Journal of the Indian Society of Remote Sensing*, vol. 44, no. 6, pp. 855–863, 2016.

[19] S. M. Vicente-Serrano, J. J. Camarero, J. M. Olano et al., "Diverse relationships between forest growth and the Normalized Difference Vegetation Index at a global scale," *Remote Sensing of Environment*, vol. 187, pp. 14–29, 2016.

[20] R. DeFries, M. Hansen, and J. Townshend, "Global discrimination of land cover types from metrics derived from AVHRR pathfinder data," *Remote Sensing of Environment*, vol. 54, no. 3, pp. 209–222, 1995.

[21] X. Chen, D. Yang, J. Chen, and X. Cao, "An improved automated land cover updating approach by integrating with downscaled NDVI time series data," *Remote Sensing Letters*, vol. 6, no. 1, pp. 29–38, 2015.

[22] F. Tian, R. Fensholt, J. Verbesselt, K. Grogan, S. Horion, and Y. Wang, "Evaluating temporal consistency of long-term global NDVI datasets for trend analysis," *Remote Sensing of Environment*, vol. 163, pp. 326–340, 2015.

[23] K. Jia, S. Liang, X. Wei et al., "Land cover classification of landsat data with phenological features extracted from time series MODIS NDVI data," *Remote Sensing*, vol. 6, no. 11, pp. 11518–11532, 2014.

[24] E. Yan, G. Wang, H. Lin, C. Xia, and H. Sun, "Phenology-based classification of vegetation cover types in Northeast China using MODIS NDVI and EVI time series," *International Journal of Remote Sensing*, vol. 36, no. 2, pp. 489–512, 2015.

[25] Z. Pan, J. Huang, Q. Zhou et al., "Mapping crop phenology using NDVI time-series derived from HJ-1 A/B data," *International Journal of Applied Earth Observation and Geoinformation*, vol. 34, no. 1, pp. 188–197, 2015.

[26] I. Nitze, B. Barrett, and F. Cawkwell, "Temporal optimisation of image acquisition for land cover classification with random forest and MODIS time-series," *International Journal of Applied Earth Observation and Geoinformation*, vol. 34, no. 1, pp. 136–146, 2015.

[27] R. Sun, Y. Rong, H. Su, and S. Chen, "NDVI time-series reconstruction based on MODIS and HJ-1 CCD data spatial-temporal fusion," *Journal of Remote Sensing*, vol. 20, no. 3, pp. 361–373, 2016.

[28] H. Ding, Z.-N. Wang, H.-J. Shang, and Y.-G. Zhang, "Climate change and its impacts on the winter wheat yield in wugong region of Shaanxi Province," *Journal of Animal and Veterinary Advances*, vol. 11, no. 20, pp. 3668–3676, 2012.

[29] Y. Shi, "Thoughts on irrigation in irrigation district of fufeng," *China Science and Technology Review*, vol. 33, pp. 497-498, 2013.

[30] S. Su, X. Zhou, C. Wan, Y. Li, and W. Kong, "Land use changes to cash crop plantations: Crop types, multilevel determinants and policy implications," *Land Use Policy*, vol. 50, pp. 379–389, 2016.

[31] S. Su, Y. Wang, F. Luo, G. Mai, and J. Pu, "Peri-urban vegetated landscape pattern changes in relation to socioeconomic development," *Ecological Indicators*, vol. 46, pp. 477–486, 2014.

[32] S. Su, C. Yang, Y. Hu, F. Luo, and Y. Wang, "Progressive landscape fragmentation in relation to cash crop cultivation," *Applied Geography*, vol. 53, pp. 20–31, 2014.

[33] V. N. Mishra, R. Prasad, P. Kumar, D. K. Gupta, and P. K. Srivastava, "Dual-polarimetric C-band SAR data for land use/land cover classification by incorporating textural information," *Environmental Earth Sciences*, vol. 76, no. 1, article 26, 2017.

[34] S.-Y. Jiang, Q.-X. Xiong, and J.-Q. Zhu, "Evaluation of lake eutrophication based on the HJ-1 satellite multispectral data," *Applied Mechanics and Materials*, vol. 519-520, pp. 1182–1185, 2014.

[35] Z. Yuan, A. Yang, and B. Zhong, "Cross comparison of the vegetation indexes between landsat TM and HJ CCD," *Remote Sensing for Land & Resources*, vol. 27, pp. 87–91, 2015.

[36] P. Hao, L. Wang, Z. Niu et al., "The potential of time series merged from Landsat-5 TM and HJ-1 CCD for crop classification: a case study for Bole and Manas Counties in Xinjiang, China," *Remote Sensing*, vol. 6, no. 8, pp. 7610–7631, 2014.

[37] P. Kumar, R. Prasad, A. Choudhary, V. N. Mishra, D. K. Gupta, and P. K. Srivastava, "A statistical significance of differences in classification accuracy of crop types using different classification algorithms," *Geocarto International*, vol. 32, no. 2, pp. 206–224, 2017.

[38] X. Li, Y. Zhang, J. Luo, X. Jin, Y. Xu, and W. Yang, "Quantification winter wheat lai with hj-1ccd image features over multiple growing seasons," *International Journal of Applied Earth Observation & Geoinformation*, vol. 44, pp. 104–112, 2016.

[39] B. Johnson, "Effects of pansharpening on vegetation indices," *ISPRS International Journal of Geo-Information*, vol. 3, no. 2, pp. 507–522, 2014.

[40] B. Lara and M. Gandini, "Assessing the performance of smoothing functions to estimate land surface phenology on temperate grassland," *International Journal of Remote Sensing*, vol. 37, no. 8, pp. 1801–1813, 2016.

[41] R. Liu, R. Shang, Y. Liu, and X. Lu, "Global evaluation of gap-filling approaches for seasonal NDVI with considering vegetation growth trajectory, protection of key point, noise resistance and curve stability," *Remote Sensing of Environment*, vol. 189, pp. 164–179, 2017.

[42] H. H. Madden, "Comments on the savitzky-golay convolution method for least-squares fit smoothing and differentiation of digital data," *Analytical Chemistry*, vol. 50, no. 9, pp. 1383–1386, 1978.

[43] W.-Y. Loh and Y.-S. Shih, "Split selection methods for classification trees," *Statistica Sinica*, vol. 7, no. 4, pp. 815–840, 1997.

[44] J. Tian, J. Wang, L. I. Yifan et al., "Land cover classification in mongolian plateau based on decision tree method: a case study in tov province, mongolia," *International Journal of Geographical Information Science*, vol. 16, pp. 460–469, 2014.

[45] F. A. Kruse, A. B. Lefkoff, J. W. Boardman et al., "The spectral image processing system (sips)-interactive visualization and analysis of imaging spectrometer data," *AIP Conference Proceedings*, vol. 283, no. 1, pp. 192–201, 1993.

[46] Y.-H. Yeh, W.-C. Chung, J.-Y. Liao, C.-L. Chung, Y.-F. Kuo, and T.-T. Lin, "Strawberry foliar anthracnose assessment by hyperspectral imaging," *Computers and Electronics in Agriculture*, vol. 122, pp. 1–9, 2016.

[47] T. He, Y.-J. Sun, J.-D. Xu, X.-J. Wang, and C.-R. Hu, "Enhanced land use/cover classification using support vector machines and fuzzy k-means clustering algorithms," *Journal of Applied Remote Sensing*, vol. 8, no. 1, Article ID 083636, 2014.

[48] N. A. Mahmon, N. Ya'Acob, and A. L. Yusof, "Differences of image classification techniques for land use and land cover classification," in *Proceedings of the IEEE 11th International Colloquium on Signal Processing and Its Applications (CSPA '15)*, pp. 90–94, Kuala Lumpur, Malaysia, March 2015.

[49] M. Baumann, M. Ozdogan, T. Kuemmerle, K. J. Wendland, E. Esipova, and V. C. Radeloff, "Using the Landsat record to detect forest-cover changes during and after the collapse of the Soviet Union in the temperate zone of European Russia," *Remote Sensing of Environment*, vol. 124, pp. 174–184, 2012.

[50] G. M. Foody, M. Pal, D. Rocchini, C. X. Garzon-Lopez, and L. Bastin, "The sensitivity of mapping methods to reference

data quality: Training supervised image classifications with imperfect reference data," *ISPRS International Journal of Geo-Information*, vol. 5, no. 11, article no. 199, 2016.

[51] H. B. Sandya, K. P. Hemanth, H. Budhiraja, and S. K. Rao, "Fuzzy rule based feature extraction and classification of time series signal," *International Journal of Soft Computing & Engineering*, vol. 3, no. 2, pp. 2231–2307, 2013.

[52] Š. Raudys and F. Roli, "The behavior knowledge space fusion method: analysis of generalization error and strategies for performance improvement," in *Proceedings of the 4th International Workshop on Multiple Classifier Systems (MCS '03)*, vol. 2709 of *Lecture Notes in Computer Science*, pp. 55–64, Springer Berlin Heidelberg, Guildford, UK, June 2003.

[53] N. Clinton, L. Yu, and P. Gong, "Geographic stacking: decision fusion to increase global land cover map accuracy," *ISPRS Journal of Photogrammetry and Remote Sensing*, vol. 103, pp. 57–65, 2015.

[54] Ş. Conţiu and A. Groza, "Improving remote sensing crop classification by argumentation-based conflict resolution in ensemble learning," *Expert Systems with Applications*, vol. 64, pp. 269–286, 2016.

[55] T. V. Tran, J. P. Julian, and K. M. De Beurs, "Land cover heterogeneity effects on sub-pixel and per-pixel classifications," *ISPRS International Journal of Geo-Information*, vol. 3, no. 2, pp. 540–553, 2014.

[56] S. Ray and L. F. Turner, "Mahalanobis distance-based two new feature evaluation criteria," *Information Sciences*, vol. 60, no. 3, pp. 217–245, 1992.

[57] S. M. Ji, L. B. Zhang, J. L. Yuan et al., "Method of monitoring wearing and breakage states of cutting tools based on Mahalanobis distance features," *Journal of Materials Processing Technology*, vol. 129, no. 1-3, pp. 114–117, 2002.

[58] A. Gasmi, C. Gomez, H. Zouari, A. Masse, and D. Ducrot, "PCA and SVM as geo-computational methods for geological mapping in the southern of Tunisia, using ASTER remote sensing data set," *Arabian Journal of Geosciences*, vol. 9, no. 20, article 753, 2016.

[59] J.-E. Ouzemou, A. El Harti, A. El Moujahid et al., "Mapping crop based on phenological characteristics using time-series NDVI of operational land imager data in Tadla irrigated perimeter, Morocco," in *Proceedings of the Remote Sensing for Agriculture, Ecosystems, and Hydrology XVII*, vol. 9637 of *SPIE Remote Sensing*, Toulouse, France, September 2015.